Tunable generation of nanometer-scale corrugations on high-index III-V semiconductor surfaces

Eric Tournié*
Max-Planck-Institut für Festkörperforschung, Heisenbergstrasse 1, D-70569 Stuttgart, Germany and Paul-Drude-Institut für Festkörperelektronik, Hausvogteiplatz 5-7, D-10117 Berlin, Germany

Richard Nötzel†
Max-Planck-Institut für Festkörperforschung, Heisenbergstrasse 1, D-70569 Stuttgart, Germany

Klaus H. Ploog
Paul-Drude-Institut für Festkörperelektronik, Hausvogteiplatz 5-7, D-10117 Berlin, Germany
(Received 12 July 1993)

We have investigated by means of *in situ* reflection high-energy electron diffraction the surface topography of various III_AIII_B-V and III-V_AV_B layers grown by solid-source molecular-beam epitaxy on (311) InP and GaAs substrates. In a wide temperature range, III_AIII_B-V (311) surfaces are corrugated on a nanometer scale in a way similar to that previously reported for (311) GaAs surfaces [R. Nötzel *et al.*, Phys. Rev. Lett. **67**, 3812 (1991)]. The geometry of the corrugations can be tuned in a well defined manner by adjusting the overlayer strain. The higher the strain is, the lower the lateral periodicity and the step height are. In addition, the surface of relaxed layers exhibits the structure of the underlying substrate. Finally, on (311)-oriented substrates the relaxation of overlayer strain at least up to 4% occurs without transition toward a three-dimensional agglomerated morphology. This indicates that the surface structure modifies the relaxation paths and mechanisms. On the other hand, the III-V_AV_B (311) surfaces are not corrugated. These results are interpreted in terms of the interplay between surface free energy, strain energy, and local-strain fields. We demonstrate that the overlayer strain is the key parameter to control the surface topography. Our work thus provides the means to directly select the interface morphology of semiconductor heterostructures.

I. INTRODUCTION

The microscopic equilibrium configuration of solid surfaces is the governing factor in a number of processes, including etching, epitaxy, and crystal growth, and is as such an important scientific issue. The configuration which will be adopted under a given set of conditions is dictated by the surface free energy of the crystal faces.[1] Simple theoretical models, taking into account only the interactions between nearest neighbors, have shown that in the case of ideal lattices nonsingular planes are unstable.[2] This finding led to the idea that planes with high surface free energy break up into faces corresponding to planes with lower surface free energy forming distinct ordered surface structures on a nanometer scale which represent the equilibrium configuration.[3] Following this idea, these nanometer surface structures could give rise to lateral confinement effects in semiconductor heterostructures and thus open an avenue for the direct synthesis of quantum wires and quantum dots during epitaxial growth.

Two approaches aiming at achieving *in situ* lateral patterning have been followed. The first one is based on investigations on the structure of and on the epitaxy on vicinal surfaces which are slightly misoriented with respect to singular planes.[4–10] This misorientation leads to the formation of monolayer-high steps separated by terraces, the width of which depends on the misorientation angle. The second approach is based on the study of high-index GaAs surfaces by Nötzel and co-workers.[3,11–13] It was shown that under molecular-beam epitaxy (MBE) growth conditions the high-index GaAs surfaces break up into planes of lower surface free energy resulting in the formation of nanometer-scale corrugations which lead to the formation of quantum-well wires during MBE growth of GaAs/AlAs heterostructures.[3,11–13] On the other hand, it was also demonstrated that the high-index GaAs surfaces flatten upon deposition of a submonolayer of highly strained materials, such as Si or InAs.[14] The question thus arises whether the transformation of high-energy high-index smooth surfaces to lower-energy corrugated configurations is unique for the "quasiperfect" GaAs/AlAs system or whether it represents a more universal feature of semiconductor and solid surfaces. Another question of importance to study is the possibility of tuning the structure of solid surfaces and by which means. Answering these questions would provide insights into the physics of solid surfaces and interfaces and shed some light on the directions to be explored from the theoretical viewpoint.

In this paper, we study the surface topography of various III-V semiconductor layers grown by solid-source MBE on (311) InP and (311) GaAs substrates by means of *in situ* reflection high-energy electron diffraction

(RHEED), which provides direct insight into the evolution of the surface structures. InP substrates exhibit a medium lattice constant among the III-V compounds and thus are well suited for the epitaxy of layers subject to a high compressive as well as tensile strain. The (311) orientation is particularly challenging because it has been demonstrated to result in the direct formation of arrays of quantum wires during MBE growth of GaAs/AlAs heterostructures.[3,11,13] For the sake of completeness, we recall in Fig. 1 the structure of the (311) GaAs surface as determined by Nötzel and co-workers[3,11–13] [Fig. 1(a)] together with the corresponding reciprocal space representation [Fig. 1(b)]. The (311) GaAs breaks up into a regular array of upward and downward steps exhibiting {331} facets with a lateral periodicity P and a step height h given in Table I. Note that this structure was not only deduced from RHEED experiments but also directly imaged by high-resolution transmission electron microscopy.[3,11]

In this work, we show that $III_A III_B$-V (311) surfaces exhibit nanometer-scale corrugations similar to the GaAs case, the geometry of which can be directly selected by the strain of the epilayer. On the other hand, III-V_A V_B surfaces exhibit a flat morphology. These results are interpreted in terms of the interplay between surface free energy, strain energy, and local-strain fields. They provide a unique means to directly selects the interface morphology of III-V semiconductor heterostructures.

The paper is organized as follows. The experiments are described in Sec. II while the experimental results are presented in Sec III and discussed in Sec. IV. Finally, Sec. V concludes the paper.

II. EXPERIMENTAL PROCEDURE

The $III_A III_B$-V samples consist of $Ga_xIn_{1-x}As$ and $Al_yIn_{1-y}As$ single layers ($0 \leq x,y, \leq 1$) grown on S-doped (311) A n-InP substrates in a Riber 2300 MBE system. To study the effect of very high strain, InAs layers were

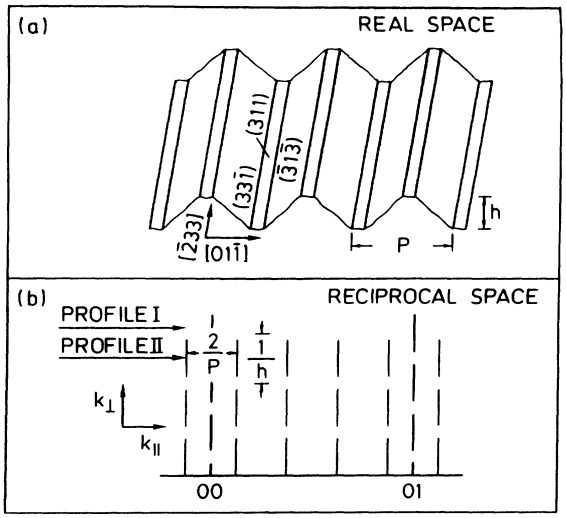

FIG. 1. Topography of the (311) surface as determined in the case of GaAs by Nötzel *et al.* (Ref. 12): (a) real space; (b) reciprocal space. The arrows in (b) indicate the positions at which intensity profiles were taken.

also grown in the same setup on Si-doped (311)A n-GaAs substrates. The III-V_A V_B samples were obtained by As_4 stabilization of InP substrates and by Sb_4 stabilization of GaAs or $Ga_{0.47}In_{0.53}As$ layers. For both the GaAs and InP substrates, the misorientation was less than 0.5°. Before introduction into the MBE system, the GaAs and InP substrates were prepared as described in Refs. 15 and 16, respectively. These methods have the advantage of a negligible etch rate and they produce (100) and (311) surfaces of comparable quality. In the MBE growth chamber, the InP substrates were heated to ≈550°C in an As_4 flux having a beam-equivalent pressure (BEP) of $BEP_{As_4} \approx (5-10)\times 10^{-6}$ Torr. The substrate temperature was then decreased to the growth temperature (be-

TABLE I. Experimental values of the lateral periodicity P (given in Å and in units of $a^{sub}_{[110]}$) and of the step height h (given in Å and in units of $a^{sub}_{[311]}$) as determined from RHEED intensity profiles for several $III_A III_B$-V systems. The error bar is ±2 Å for h and ±5 Å for P.

Epilayer/Substrate	Strain (%)	P(Å/$a^{sub}_{[110]}$)	h(Å/$a^{sub}_{[311]}$)
Lattice-matched systems:			
GaAs/GaAs	0	32/8	10/6
$Ga_{0.47}In_{0.53}As$/InP	0	43/10	9/5
$Al_{0.48}In_{0.52}As$/InP	0	42/10	9/5
Strained systems:			
InAs/$Ga_{0.47}In_{0.53}As$	3.2	26/6	6/3
InAs/InP	3.2	25/6	5/3
GaAs/$Ga_{0.47}In_{0.53}As$	−3.9	25/6	5/3
InAs/GaAs	7.2	0	0
Relaxed systems:			
InAs/$Ga_{0.47}In_{0.53}As$	0	39/9	7.5/4
GaAs/$Ga_{0.47}In_{0.53}As$	0	37/9	8.5/5
InAs/GaAs	0	34/8	9/5

tween 450 °C and 550 °C for different samples) before starting the growth of either $Ga_xIn_{1-x}As$ or $Al_yIn_{1-y}As$ at a growth rate of 2.2 Å/s. The As_4 flux was kept constant for all the growth runs and the As_4/group-III flux ratio was ≈ 10. The GaAs oxide, on the other hand, was desorbed by heating the substrates in an As_4 flux of the same BEP_{As_4} up to ≈ 580 °C. GaAs buffer layer was then grown at a temperature ranging from 580 to 620 °C in different runs and a growth rate of 2.8 Å/s. Subsequently, InAs layers of various thickness were deposited at ≈ 420 °C with a growth rate of 1.2 Å/s. The *in situ* substrate preparations as well as the growth runs were monitored by RHEED using grazing incident (angle of incidence $\approx 1°$) 20 keV electrons. For further analysis, the RHEED patterns were recorded by a CCD camera connected to an image processing system. The transverse RHEED profiles were taken close to out-of-phase conditions.

III. EXPERIMENTAL RESULTS

We first present the results obtained with the arsenide layers and then those with the III-V_A V_B compounds. In Fig. 2 we show the RHEED patterns taken 5 min after the end of the growth of a 50-nm-thick $Ga_{0.47}In_{0.53}As$ layer (lattice matched to InP) at 500 °C. The pattern observed along the $[01\bar{1}]$ azimuth shows a pronounced streaking [Fig. 2(a)] indicating a high density of steps oriented along the perpendicular $[\bar{2}33]$ direction. Indeed, along the $[\bar{2}33]$ azimuth [Fig. 2(b)] we observe a pattern characteristic of a two-level system composed of upward and downward steps.[17] The streaks are split into satellites, or unsplit depending on the scattering vector $k_\perp$, i.e., on the position along the length of the streaks. Moreover, the intensity maximum of the main streak corresponds to an intensity minimum of the satellites and vice versa. Since the RHEED pattern displayed in Fig. 2(b) directly images the reciprocal lattice shown in Fig. 1(b), the step height h and the lateral periodicity P can be directly determined from the splitting along the streaks and from the separation of the satellites, respectively.[17] All the information regarding the geometry of the step system is contained in the RHEED pattern taken along the azimuth parallel to the steps, i.e., the $[\bar{2}33]$ azimuth in our case, and we will focus on it in the following. The error bar, mainly due to the resolution of our image processing system, for all values given hereafter, is evaluated to ± 2 Å for h and ± 5 Å for P. In Figs. 3(a) and 3(b) the intensity profiles taken through the pattern of Fig. 2(b) at the positions corresponding to the arrows marked I and II in Fig. 1(b), respectively, are displayed. These profiles are indeed characteristic of a two-level step system.[17] From the satellite separation in Fig. 3(b) we deduce a lateral periodicity of 43 Å, i.e., $10a^{InP}_{[110]}$. The splitting along the main streak gives a step height of 9 Å, i.e., $5a^{InP}_{[311]}$. The same RHEED patterns are obtained from $Al_{0.48}In_{0.52}As$ layers (also lattice matched to InP), and the transverse intensity profile displayed in Fig. 3(c) reveals that the periodicity is the same as with $Ga_{0.47}In_{0.53}As$ grown on InP. Both the $Ga_{0.47}In_{0.53}As$ and $Al_{0.48}In_{0.52}As$ surface structures are stable in the wide temperature range between 300 °C and 550 °C. The RHEED pattern observed along the $[\bar{2}33]$ azimuth during MBE growth of either $Ga_{0.47}In_{0.53}As$ or $Al_{0.48}In_{0.52}As$ is depicted in Fig. 4(a). The pattern is more diffuse than that obtained from a static surface [Fig. 2(b)]. However, the RHEED intensity profile taken along the main streak [Fig. 4(b)] reveals its split nature and the average spacing between the maxima gives a step height of 8.5 Å, which indicates that the corrugated surface structure is preserved during growth. Upon growth interruption the RHEED pattern returns toward the equilibrium case displayed in Fig. 2(b) in a few minutes. It is finally important to note that the RHEED patterns presented above can already be clearly observed from epilayers only a few nanometers thick.

The RHEED patterns observed from strained $Ga_xIn_{1-x}As$ as well as $Al_yIn_{1-y}As$ ternary layers grown on (311) InP substrates are qualitatively the same as those obtained from lattice-matched layers, although somewhat more diffuse unless for the highly strained InAs and

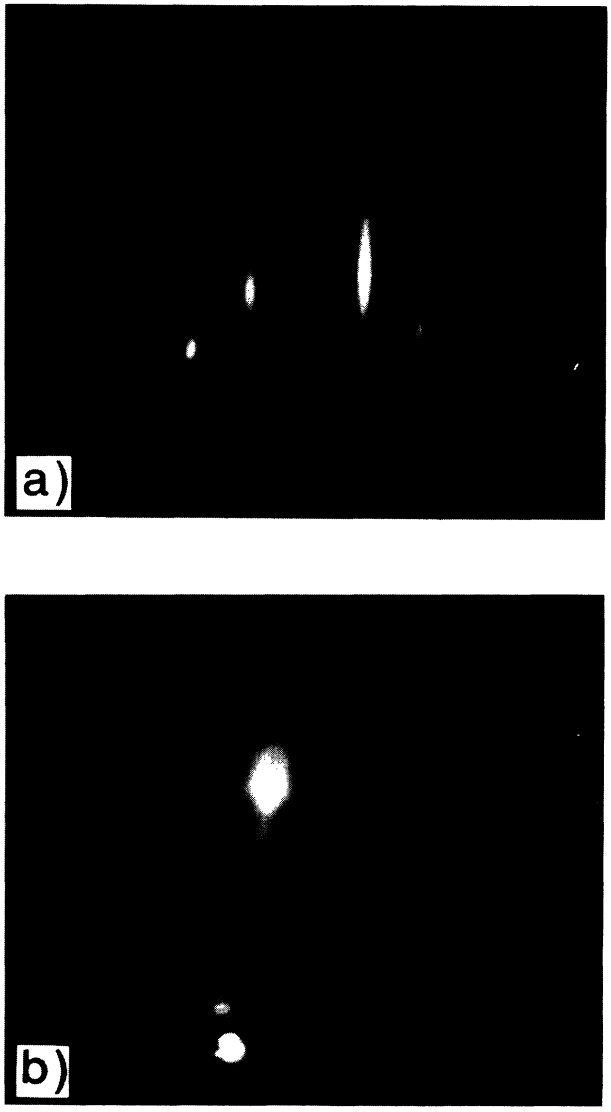

FIG. 2. RHEED patterns taken from a $Ga_{0.47}In_{0.53}As$ layer grown on (311) InP: (a) $[01\bar{1}]$ azimuth; (b) $[\bar{2}33]$ azimuth.

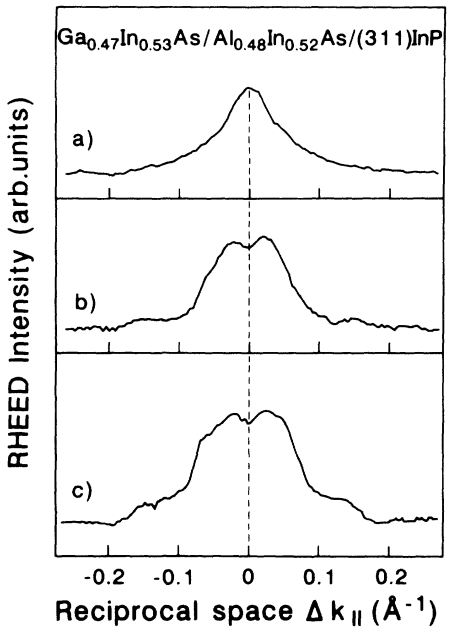

FIG. 3. Transverse intensity-profiles taken through the [$\bar{2}33$] RHEED patterns: (a) as indicated by arrow I in Fig. 1(b) for a $Ga_{0.47}In_{0.53}As$ layer; (b) as indicated by arrow II in Fig. 1(b) for a $Ga_{0.47}In_{0.53}$ layer, and (c) as indicated by arrow II in Fig. 1(b) for an $Al_{0.48}In_{0.52}As$ layer.

GaAs binary compounds. However, a very important characteristic is that the lateral periodicity and the step height change continuously when going from the lattice-matched ternary materials toward the binary extremes. As an example, we show in Fig. 5(a) the transverse intensity profile through the RHEED pattern observed along the [$\bar{2}33$] azimuth from a 6-Å-thick strained ($\epsilon=3.2\%$) InAs layer deposited on a (311)-$Ga_{0.47}In_{0.53}As$ buffer layer. From the satellite separation, we deduce a lateral periodicity of $P\approx 26$ Å$\approx 6a^{InP}_{[110]}$. The step height is determined to be $h\approx 6$ Å$\approx 3a^{InP}_{[311]}$. Similar values are obtained from strained GaAs layers ($\epsilon=-3.9\%$) on (311) $Ga_{0.47}In_{0.53}As$ or $Al_{0.48}In_{0.52}As$ buffer layers (Table I). In addition, we have observed that the surfaces flatten upon deposition of a monolayer-thick highly strained ($\epsilon=7.2\%$) InAs film on a (311) GaAs substrate as was reported previously.[14] In another set of experiments we have investigated the surface structure of relaxed GaAs layers grown on $Ga_{0.47}In_{0.53}As$ or $Al_{0.48}In_{0.52}As$ buffer layers and of *relaxed* InAs layers grown on either (311) $Ga_{0.47}In_{0.53}As$ (or $Al_{0.48}In_{0.52}As$) or (311) GaAs buffer layers. Figure 5(b) shows the RHEED intensity profile taken from a 0.5-μm-thick relaxed InAs layer on a (311) GaAs buffer layer. The striking feature is that the relaxed layer exhibits a surface structure which is quasi-identical to the structure of the underlying buffer layer (Table I), although strain-relieving defects are present. As for the case of GaAs grown onto a (311) GaAs substrate,[3,11,13] the corrugated surface structures of both InAs and GaAs relaxed layers are stable upon cooling down to room temperature.

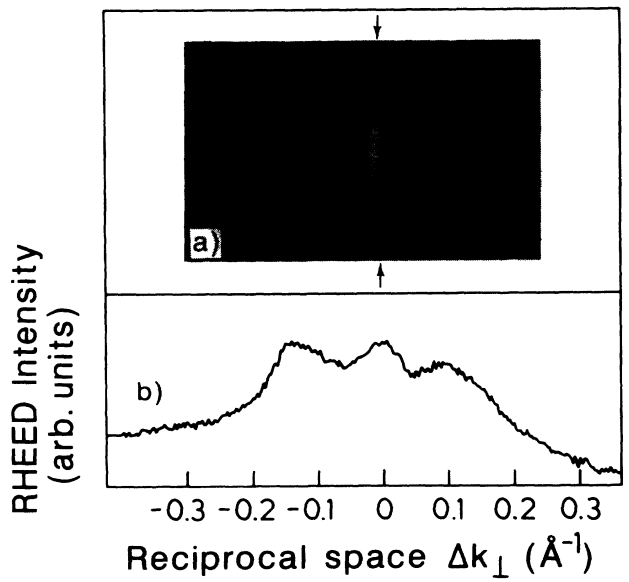

FIG. 4. (a) RHEED pattern taken along the [$\bar{2}33$] azimuth from a growing $Ga_{0.47}In_{0.53}As$ layer, and (b) RHEED intensity profile along the main streak, as indicated by the inward arrows in (a). The horizontal scale refers to (b) only.

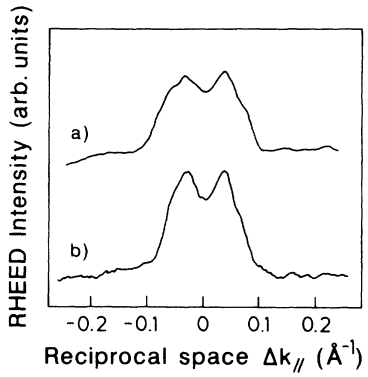

FIG. 5. Transverse intensity-profiles taken through the [$\bar{2}33$] RHEED patterns: (a) as indicated by arrow II in Fig. 1(b) for an InAs layer strained onto a (311) $Ga_{0.47}In_{0.53}As$ buffer layer; (b) as indicated by arrow II in Fig. 1(b) for a relaxed InAs layer grown onto a (311) GaAs buffer layer.

We wish to point out here that, in contrast to our observation on (100)-oriented InP substrates even with lattice-matched layers,[18] upon growth initiation onto the (311)-oriented InP substrate the RHEED pattern does not exhibit any spotty 3D feature. In addition, when MBE growth is carried out onto (311)-oriented InP substrates, the strain relaxation proceeds without growth-mode transition toward a 3D agglomerated morphology,[19] even for the high strain values of 3.2% (InAs on InP) and -3.9% (GaAs on InP) achieved here. On the other hand, during MBE growth of InAs onto (311)-oriented GaAs (7.2% strain) islanding is observed at a thickness ranging between 5 and 6 Å, a value similar to what is obtained on (100)-oriented GaAs.[20] This result points to the fact that, depending on the magnitude of the

strain, the surface orientation, i.e., the surface structure, drastically affects the strain-relaxation path and mechanism. This phenomenon has not yet been investigated, either experimentally or theoretically, and hence represents an additional challenge before achieving a complete understanding of the intricate fundamentals at work in the exciting, albeit complex, field of strain-layer epitaxy.

As a final set of data, we show in Fig. 6 the RHEED patterns taken along the $[01\bar{1}]$ azimuth [Fig. 6(a)] and along the $[\bar{2}33]$ azimuth [Fig. 6(b)] from the (311) InP surface stabilized in an As_4 flux at 500 °C. These patterns were taken immediately after oxide desorption. Long streaks can be seen in both directions, which indicate the absence of surface corrugations. However, upon long annealing (30 min) of the InP substrate in an As_4 flux, the RHEED pattern evolves and eventually the surface corrugations develop. The lateral periodicity and step height are then very close to the values measured in the case of InAs strained onto $Ga_{0.47}In_{0.53}As$ (Table I). Finally, a typical RHEED pattern observed along the $[\bar{2}33]$ azimuth from Sb_4-stabilized (311) GaAs or $Ga_{0.47}In_{0.53}As$ surfaces is displayed in Fig. 7. The well resolved twofold reconstruction reveals also the absence of corrugations.

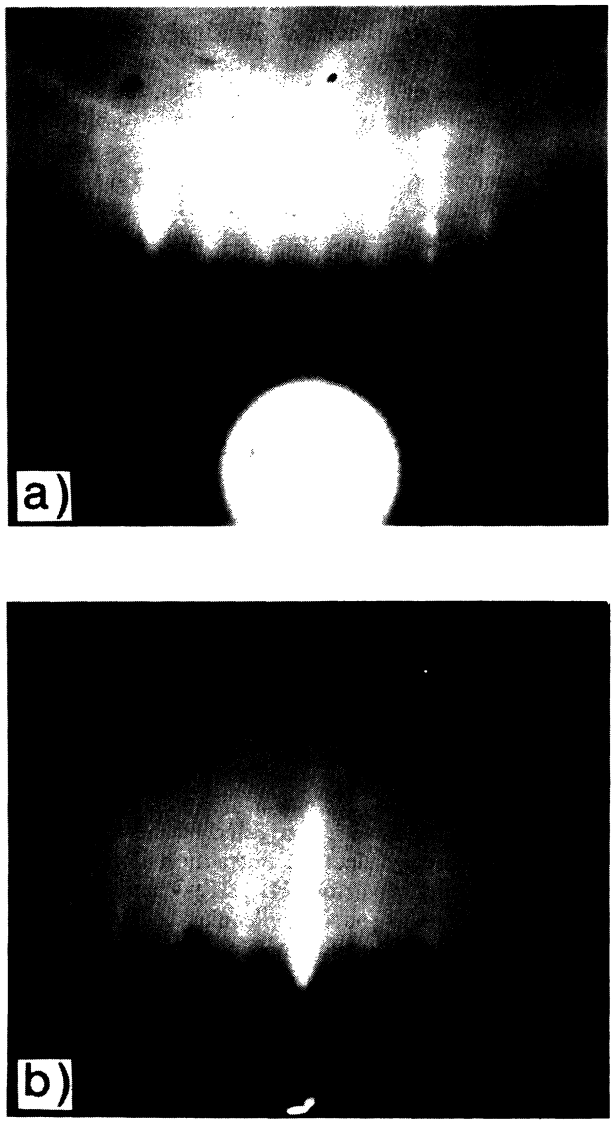

FIG. 6. RHEED patterns taken from the As_4-stabilized (311) InP substrate immediately after oxide desorption: (a) $[01\bar{1}]$ azimuth; (b) $[\bar{2}33]$ azimuth.

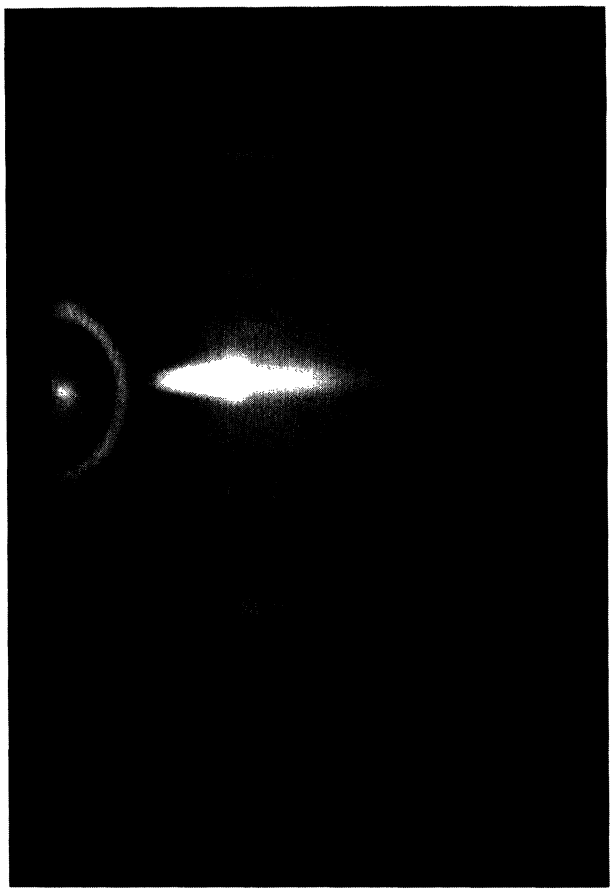

FIG. 7. RHEED pattern taken along the $[\bar{2}33]$ azimuth from the Sb_4-stabilized (311) GaAs surface.

IV. DISCUSSION

The important result is that the RHEED patterns obtained from arsenide layers are identical to those observed with (311) GaAs surfaces.[3,11–13] The (311) surfaces of $Ga_xIn_{1-x}As$ and Al_yIn_{1-y} layers thus exhibit the same corrugated structure as the one displayed in Fig. 1(a). However, the crucial feature to be noted here is that the lateral periodicity P and the step height h can be tuned in a well defined manner by selecting the proper epilayer/substrate combination and/or the overlayer strain (Table I). This finding is a direct consequence of the equilibrium nature of the corrugated surface, the driving force behind the formation of a "hill-and-valley" structure being the quest for the energetically most favorable configuration.[21] In this context the key parameter is the ratio $\Gamma=\gamma_{\{331\}}/\gamma_{\{311\}}$, where $\gamma_{\{hkl\}}$ is the free energy of the $\{hkl\}$ surface. Theoretical studies have indeed shown that $\Gamma<1$ in the case of Si surfaces,[22] but to our knowledge similar studies have not yet been performed

for compound semiconductors. For these materials, the calculations are rendered very difficult by the necessity to account for the influence of the surface reconstructions and of the nonequivalent polar surfaces. In the case of strained epilayers, an additional strain-energy term, including an important shear-strain component,[23] has to be taken into account. The study of InAs grown onto (311) GaAs illustrates the dramatic influence of the strain energy on the energy balance. In fact, for a strained film the surface is flat while it is corrugated for a relaxed film. Consequently, the global energy balance depends not only on the orientation but also on the peculiarities of each materials system, which then adopts its own topography.

The diffuse RHEED pattern observed during growth, which is more pronounced with $Al_yIn_{1-y}As$ than with $Ga_xIn_{1-x}As$, can be understood by the same arguments since during growth the equilibrium is, by essence, not achieved. Consequently, upon growth interruption a few-minutes annealing (depending on the temperature) is required for the atoms to find their proper lattice site, i.e., a temporal evolution of the RHEED pattern is observed which reflects the dynamic recovery of the surface configuration toward the equilibrium state. In addition, we deal here with the epitaxy of ternary alloys, solid solutions of very different and highly mismatched binary compounds, namely GaAs and InAs on the one hand and AlAs and InAs on the other hand. During MBE growth, the random occupation of the cation lattice sites implies that local alloy fluctuations are unavoidable. In turn, this results in high local-strain fields and bond distortion, which change the local energy balance. The detrimental influence of these local-strain fields on the orderings of the surface manifests itself in the intensity profiles displayed in Figs. 3(b) and 3(c). Indeed, even for *lattice-matched* ternary layers the minima of the main streak ($\Delta k_{\parallel}=0$) are much shallower than those obtained with an InAs film, either strained onto $Ga_{0.47}In_{0.53}As$ [Fig. 5(a)] or relaxed onto GaAs [Fig. 5(b)]. As a consequence, while a perfect corrugated surface is obtained after only a few seconds anneal during MBE growth of GaAs/AlAs structures,[3,11,13] a longer annealing time is needed with the ternary materials to reach the equilibrium. Furthermore, as compared to $Ga_xIn_{1-x}As$, even the growth of high quality (100) $Al_yIn_{1-y}As$ is plagued by several problems,[18] mainly due to the much lower mobility of Al adatoms as compared to Ga adatoms. This explains why the $Al_yIn_{1-y}As$ surface is more disordered than its $Ga_xIn_{1-x}As$ counterpart during growth and consequently its RHEED pattern is more diffuse.

The data obtained with the As_4-stabilized (311) InP and Sb_4-stabilized (311) GaAs and $Ga_{0.47}In_{0.53}As$ surfaces complement and confirm the conclusions drawn above. In fact, one has to bear in mind that during the stabilization process part of the surface group-V atoms undergoes an exchange with atoms of the impinging flux. In our particular case, this results in the formation of In(As)(P),[24–27] Ga(As)(Sb), and GaIn(As)(Sb) (Refs. 28 and 29) surface layers. We emphasize here that the stabilization process leads to true epitaxial layers and is not simply a reconstruction effect.[30] In fact, the presence of streaky RHEED patterns indicates that the absence of corrugations does not stem from a low quality surface, which would result in a spotty pattern, but is an intrinsic property of these layers. Two important features of these layers can explain the absence of corrugations. First, at least one of their sublattices is shared among two species, which leads to local fluctuations and local-strain fields. Second, these surface layers are highly strained. The first effect manifests itself in the annealing behavior of the (311) InP surface. Indeed, upon long annealing in an As_4 flux, a layer of pure InAs progressively develops on the InP surface.[24] Consequently, the disorder and local fluctuations disappear. The As_4-stabilized InP surface consists finally in a strained ($\epsilon=3.2\%$) InAs film on an InP substrate. At this time, we observe an evolution of the RHEED pattern which eventually reveals a corrugated surface. Note that the lateral periodicity and step height are, within the error bar, similar to the values measured from strained InAs films grown on $Ga_{0.047}In_{0.53}As$ layers which are subject to the same strain ($\epsilon=3.2\%$). As for the second point, careful inspection and comparison of Figs. 6(b) and 7 are necessary. Strikingly, the RHEED pattern displayed in Fig. 7 is much better resolved and intense than the one of Fig. 6(b). In addition, the pattern of Fig. 7, observed along the $[\bar{2}33]$ azimuth, exhibits a perfect twofold reconstruction which well agrees with the classical description of the noncorrugated (311) surface being composed of (100) treads and (111) risers.[31] The maximum possible average strain as well as local strain are much higher in the case of a GaAs surface stabilized by Sb_4 (Fig. 7) than in the case of an InP surface stabilized by As_4 [Fig. 6(b)]. In addition to the case of InAs deposited onto (311) GaAs described above, this latter result demonstrates unambiguously that the strain, via its influence on the energy balance of the system, is the key parameter which controls the surface topography. In addition, local fluctuations play also a decisive role in the case of alloy materials and should be accounted for.

Finally, our results clearly demonstrate that more theoretical work is needed to assess the different contributions to the energy balance of solid surfaces before the ultimate goal of an *a priori* prediction of the equilibrium surface structure of a given system can be achieved.

V. CONCLUSION

In conclusion, we have investigated by means of *in situ* reflection high-energy electron diffraction (RHEED) the surface topography of various III_AIII_B-V and III-V_AV_B layers grown by solid-source molecular-beam epitaxy on (311) InP and GaAs substrates. In a wide temperature range, III_AIII_B-V (311) surfaces are corrugated on a nanometer scale with a lateral periodicity and a step height which can be tuned in a well defined manner by adjusting the overlayer strain. In addition, the surface of relaxed layers exhibits the structure of the underlying substrate. Finally, on (311)-oriented substrates the relaxation of overlayer strain at least up to 4% occurs without transition toward a 3D agglomerated morphology, which indicates that the surface structure modifies the relaxa-

tion paths and mechanisms. On the other hand, the III-V_A V_B (311) surfaces are flat and reconstructed. These results are interpreted in terms of the interplay between surface free energy, strain energy, and local-strain fields and we demonstrate that the overlayer strain is the key parameter to control the surface topography. Finally, the results obtained with relaxed layers demonstrate that the epilayer/substrate combination can arbitrarily and most conveniently be selected without impairing the feasibility of natural corrugations.

ACKNOWLEDGMENTS

Part of this work was sponsored by the GSI Darmstadt and by the Bundesministerium für Forschung und Technologie of the Federal Republic of Germany.

*Present address: L.P.S.E.S./C.N.R.S., Parc Sophia Antipolis, F-06560 Valbonne, France.

†Present address: NTT-Optoelectronics Laboratories, Atsughishi, Kanagawa 243-01, Japan.

[1]E. D. Williams and N. C. Bartelt, Science **251**, 393 (1991).

[2]C. Herring, in *Structure and Properties of Solid Surfaces,* edited by R. Gomer and C. S. Smith (American Institute of Mineralogical and Metallurgical Engineers, Chicago, 1952), p. 51.

[3]R. Nötzel, L. Däweritz, and K. Ploog, Phys. Rev. B **46**, 4736 (1992).

[4]P. M. Petroff, A. C. Gossard, and W. Wiegmann, Appl. Phys. Lett. **45**, 620 (1984).

[5]P. R. Pukite, G. S. Petrich, S. Batra, and P. I. Cohen, J. Cryst. Growth **95**, 269 (1989).

[6]T. Fukui and H. Saito, Jpn. J. Appl. Phys. **29**, L731 (1990).

[7]M. Tanaka, J. Motohisa, and H. Sakaki, Surf. Sci. **228**, 408 (1990).

[8]M. S. Miller, H. Weman, C. E. Pryor, M. Krishnamurthy, P. M. Petroff, H. Kroemer, and J. L. Merz, Phys. Rev. Lett. **68**, 3464 (1992).

[9]T. Shitara, D. D. Vvdensky, M. R. Wilby, J. Zhang, J. H. Neave, and B. A. Joyce, Phys. Rev. B **46**, 6815 (1992).

[10]M. Kasu and N. Kobayashi, Appl. Phys. Lett. **62**, 1262 (1993).

[11]R. Nötzel, N. N. Ledentsov, L. Däweritz, M. Hohenstein, and K. Ploog, Phys. Rev. Lett. **67**, 3812 (1991).

[12]R. Nözel, N. N. Ledentsov, L. Däweritz, M. Hohenstein, and K. Ploog, Phys. Rev. B **45**, 3507 (1992).

[13]R. Nötzel and K. Ploog, J. Vac. Sci. Technol. A **10**, 617 (1992).

[14]M. Ilg, R. Nözel, K. H. Ploog, and M. Hohenstein, Appl. Phys. Lett. **62**, 1472 (1993).

[15]H. Fronius, A. Fischer, and K. Ploog, Jpn. J. Appl. Phys. **25**, L137 (1986).

[16]E. Tournié, L. Tapfer, T. Bever, and K. Ploog, J. Appl. Phys. **71**, 1790 (1992).

[17]M. G. Lagally, D. E. Savage, and M. C. Tringides, in *Reflection High-Energy Electron Diffraction and Reflecting Electron Imaging of Surfaces,* Vol. 188 of *NATO Advanced Study Institute Series B: Physics,* edited by P. K. Larsen and P. J. Dobson (Plenum, New York, 1988), p. 139.

[18]E. Tournié, Y.-H. Zhang, N. J. Pulsford, and K. Ploog, J. Appl. Phys. **70**, 7362 (1991).

[19]C. W. Snyder, B. G. Orr, D. Kessler, and L. M. Sander, Phys. Rev. Lett. **66**, 3032 (1991).

[20]O. Brandt, K. Ploog, L. Tapfer, M. Hohenstein, R. Bierwolf, and F. Phillipp, Phys. Rev. B **45**, 8443 (1992).

[21]C. Herring, Phys. Rev. **82**, 87 (1951).

[22]D. J. Chadi, Phys. Rev. B **29**, 785 (1984).

[23]L. De Caro and L. Tapfer, Phys. Rev. B **48**, 2298 (1993).

[24]J. M. Moison, M. Bensoussan, and F. Houzay, Phys. Rev. B **34**, 2018 (1986).

[25]G. Hollinger, D. Gallet, M. Gendry, G. Santinelli, and P. Viktorovitch, J. Vac. Sci. Technol. B **8**, 832 (1990).

[26]C. Giannini, L. Tapfer, E. Tournié, Y. H. Zhang, and K. H. Ploog, Appl. Phys. Lett. **62**, 149 (1993).

[27]E. Carlino, M. Catalano, C. Giannini, L. Tapfer, E. Tournié, Y. H. Zhang, and K. H. Ploog, in the *8th Oxford Conference on the Microscopy of Semiconductor Materials,* edited by A. Cullis, IOP Conf. Proc. No. 134 (Institute of Physics and Physical Society, London, 1993), p. 21.

[28]M. Yano, M. Ashida, A. Kawaguchi, Y. Iwai, and M. Inoue, J. Vac. Sci. Technol B **7**, 199 (1989).

[29]M. Yano, H. Yokose, Y. Iwai, and M. Inoue, J. Cryst. Growth **111**, 609 (1991).

[30]Photoluminescence characterizations of layers grown by substrate stabilization have indeed been reported. See, e.g., Ref. 24 and Z. Sobiesierski *et al.*, Appl. Phys. Lett. **58**, 1863 (1991).

[31]R. C. Sangster, in *Compound Semiconductors,* edited by R. K. Willardson and H. L. Goering (Reinhold, New York, 1962), Vol. 1, p. 241.

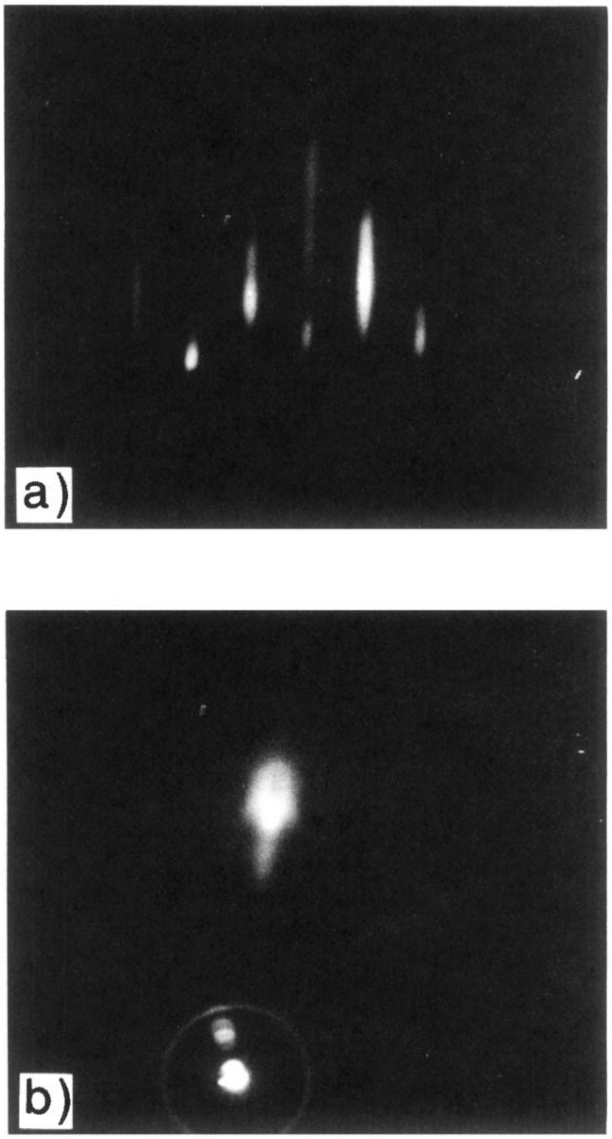

FIG. 2. RHEED patterns taken from a $Ga_{0.47}In_{0.53}As$ layer grown on (311) InP: (a) $[01\bar{1}]$ azimuth; (b) $[\bar{2}33]$ azimuth.

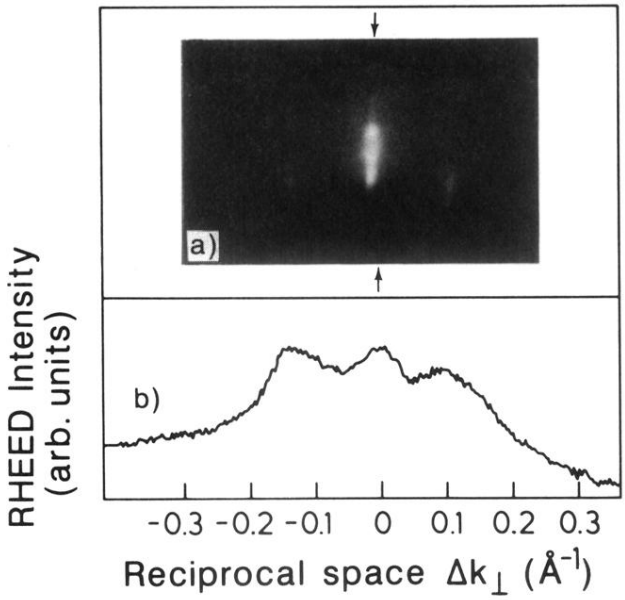

FIG. 4. (a) RHEED pattern taken along the [$\bar{2}33$] azimuth from a growing $Ga_{0.47}In_{0.53}As$ layer, and (b) RHEED intensity profile along the main streak, as indicated by the inward arrows in (a). The horizontal scale refers to (b) only.

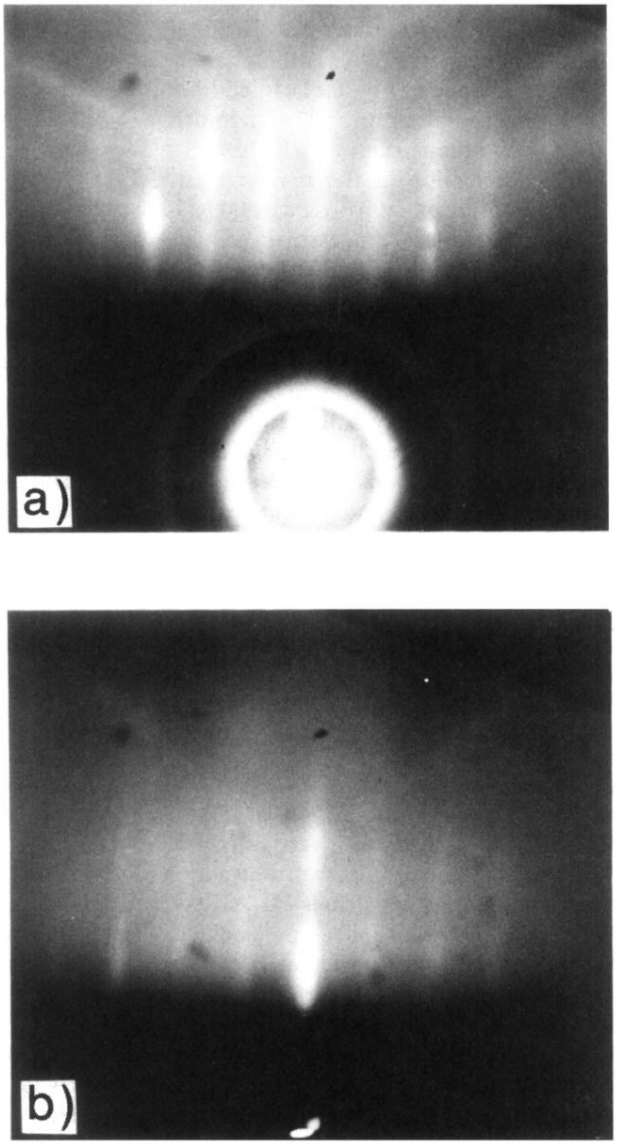

FIG. 6. RHEED patterns taken from the As_4-stabilized (311) InP substrate immediately after oxide desorption: (a) $[01\bar{1}]$ azimuth; (b) $[\bar{2}33]$ azimuth.

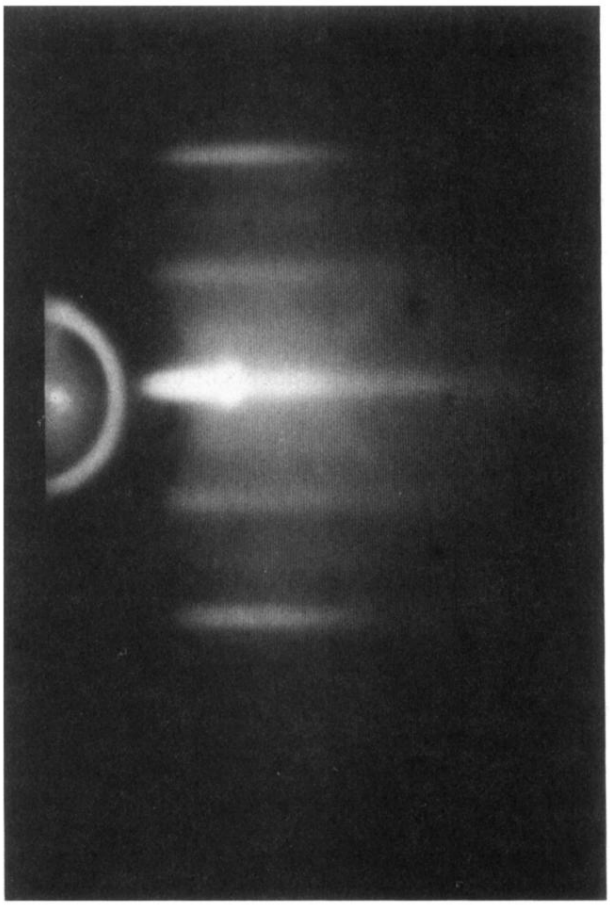

FIG. 7. RHEED pattern taken along the [$\bar{2}$33] azimuth from the Sb_4-stabilized (311) GaAs surface.